Article:
Fletcher, P., Martínez de Arriba, G., Tian, Y. et al. (5 more authors) (2022) Optical characterisation of InGaN-based microdisk arrays with nanoporous GaN/GaN DBRs. Journal of Physics D: Applied Physics, 55 (46). 464001. ISSN 0022-3727

https://doi.org/10.1088/1361-6463/ac8fa0

Optical characterisation of InGaN-based microdisk arrays with nanoporous GaN/GaN DBRs

OPEN ACCESS
IOP Publishing
Journal of Physics D: Applied Physics
J. Phys. D: Appl. Phys. **55** (2022) 464001 (7pp)
https://doi.org/10.1088/1361-6463/ac8fa0

Optical characterisation of InGaN-based microdisk arrays with nanoporous GaN/GaN DBRs

Peter Fletcher[1], **Guillem Martínez de Arriba**[1], **Ye Tian, Nicolas Poyiatzis, Chenqi Zhu, Peng Feng, Jie Bai and Tao Wang***

Department of Electronic and Electrical Engineering, The University of Sheffield, Sheffield S1 3JD, United Kingdom

E-mail: t.wang@sheffield.ac.uk

Received 11 May 2022, revised 29 August 2022
Accepted for publication 6 September 2022
Published 23 September 2022

Abstract

Optically pumped whispering gallery mode (WGM) lasing has been observed in many freestanding microdisk structures. Dry etching is normally used to fabricate the microdisks, which causes severe sidewall damage, resulting in degradation of lasing performance, especially for ultra-small electrically-injected devices. In this paper, we demonstrate high quality microdisk cavities with 3.5 μm diameter, by combining a selective overgrowth approach and an epitaxial lattice-matched distributed Bragg reflector (DBR), topped with a highly reflective (>99%) dielectric DBR. InGaN polaritons are found to occur in the high-quality microcavities. WGM modes are measured, with the positions in good agreement with finite difference time domain simulations. Furthermore, lasing behaviour is observed with a threshold at 410 μW and a dominant mode at 488 nm.

Supplementary material for this article is available online

Keywords: InGaN, microdisk, nanoporous, optical characterisation, DBR

(Some figures may appear in colour only in the online journal)

1. Introduction

III–V semiconductor micro-cavities have attracted large interest for their application in high performance optoelectronic devices [1, 2]. In particular, GaN-based microdisk lasers are gaining increasing attention due to its large tuneable potential band gap range covering from Ultraviolet to visible light [2], high quantum efficiency [3], and ultra-low threshold of lasers [4]. Many recent works have focused on making microdisk lasers by forming a GaN-air cavity with freestanding structures [5, 6]. The microcavity structures are usually fabricated by means of dry-etching processes, which produces surface damage on side walls. It will result in enhanced non-radiative recombination and degradation in optical performance [7]. The issue becomes more severe with decreasing the dimension of microdisks due to the large surface-to-volume ratio [8]. Though lots of research has been carried out to reduce plasma-induced damage through passivation using dielectric materials such as SiO_2, the issue remains severe, especially for electrically-driven devices due to unavoidable current leakage and degraded electrical injection [9, 10]. Moreover, it is a challenge to integrate the microcavities into electronic devices due

[1] These authors contributed equally to this work.
* Author to whom any correspondence should be addressed.

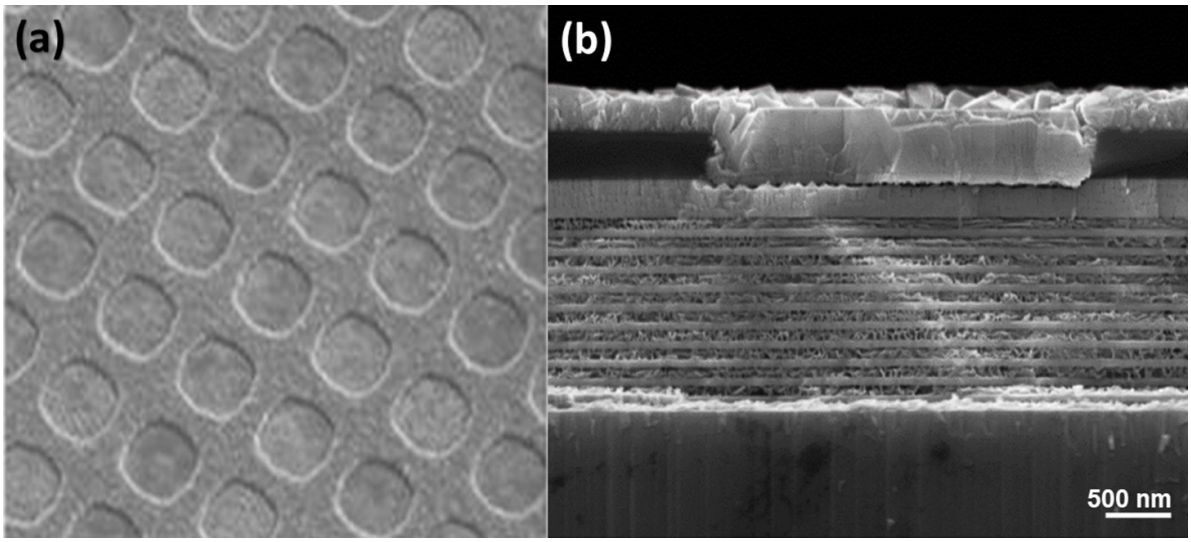

Figure 1. (a) Top down SEM image of the array structure (b) cross-sectional SEM of the nanoporous InGaN/GaN distributed Bragg reflectors.

to their delicate nature. While such electrically-driven lasers haven been realised, the reports show that only single microdisk can be excited at one time [10–13].

Recently, a different approach to creation of InGaN-based micro light-emitting diodes (μLEDs) is developed [4, 14]. By employing a selectively overgrowth method, the μLEDs can be formed inside a GaN micro-hole array with a SiO_2 mask. Compared to conventional etching methods, it can avoid the plasma-induced damage to side walls. Furthermore, the SiO_2 mask provides an easy way to achieve micro-devices based on the overgrown microdisk array epi-wafers.

To develop these devices into a vertical cavity surface emitting laser (VCSEL), high performance distributed Bragg reflectors (DBRs) will be required. Recently, nanoporous GaN (NP-GaN) have been reported as a method to create high reflectance lattice-matched GaN DBRs [8, 15–17]. It offers an alternative to other epitaxial GaN-based DBRs that usually require many pairs of alternating layers before achieving desired results such as AlGaN/GaN [18]. In this paper, we will demonstrate high quality InGaN-based microdisk cavities with 3.5 μm diameter, which includes a bottom NP-GaN DBR and a top dielectric DBR. Optically-pumped whispering gallery modes (WGM) have been measured and lasing behaviour is obtained with a threshold at 410 μW and a dominant mode at 488 nm.

2. Experiments

Our InGaN-based micro-disk arrays are grown on a patterned GaN template by metal organic vapour phase epitaxy (MOVPE). First, the GaN template is grown on a c-plane sapphire substrate using a standard two-step growth method using MOVPE. It starts with a undoped GaN layer and 11 pairs of alternating highly silicon doped n-type GaN (n-GaN)/undoped-GaN (u-GaN) DBR, followed by a 600 nm n-GaN layer with a doping level of 5×10^{19} cm^3. Then a SiO_2 dielectric layer is deposited on top of the as-grown template, approximately 500 nm thick, using a standard plasma enhanced chemical vapour deposition technique. Afterwards, the template is then patterned by photolithography and etched down to the n-GaN layer, using inductively coupled plasma to create micro-hole arrays with a diameter of 3.6 μm and an interpitch of 2 μm. Finally, the patterned template is put into the MOVPE again for further growth of an InGaN/GaN light-emitting diode (LED) structure. It is composed of a starting n-GaN layer, an InGaN pre-layer with 5% indium content, and five periods of multi quantum wells (MQWs) with 2.5 nm InGaN well and 13.5 nm GaN barrier, topped with a 20 nm p-type $Al_{0.2}Ga_{0.8}N$ layer and a final 200 nm p-type GaN layer. Due to the SiO_2 dielectric mask, the overgrowth only happens in the micro-holes, forming an array of grown μLEDs, as shown in figure 1(a). Through modifying the diameter and interpitch of photomasks, micro-LED arrays with different sizes can be grown.

In order to form a lattice-matched DBR structure from the highly doped n-GaN/u-GaN layers, electrochemical-etching (EC) is performed on the μLED array sample. The EC process is conducted in 0.3 M nitric acid at 6 V bias for 30 mins, with the μLED sample as an anode and a Pt plate as cathode. Figure 1(b) is a typical scanning electron microscopy (SEM) image of an EC-etched microdisk sample. It can be seen clearly that the highly doped n-GaN layers have become nanoporous. There is a large difference in the refractive indices between the NP-GaN layer and the u-GaN layer, which results in a high reflectivity of the lattice-matched DBR. To finally form a VCSEL cavity, a dielectric lambda quarter DBR is deposited on top of the μLEDs composed of six pairs of SiO_2/SiN layers. In this work, 3D finite difference time domain (FDTD) simulations are used to help design the high quality microcavity. The thicknesses of each layer for the dielectric DBR, with 85 nm for SiO_2 and 61 nm for SiN, are supposed to be most effective by means of FDTD simulations.

3. Results and discussion

To achieve high quality cavities with lasing behaviour, microdisks need to be formed, because strong coupling between the photons and excitons is expected to form in such structures, creating exciton polaritons [19, 20]. However, it is difficult to observe exciton polaritons in InGaN MQWs due to the large inhomogeneity broadening [21]. Therefore, to enhance the lasing chances, the structure has been designed to obtain a large stopband for a greater wavelength range of modes, allowing a greater chance of polaritons to be observed.

Figure 2 shows reflectance of the microcavity along with two respective DBRs: one is an EC-formed lattice-matched NP-GaN/GaN DBR, and the other one is a dielectric DBR deposited on sapphire. As shown in figure 2, both the NP-GaN/GaN DBR and the dielectric DBR have central wavelengths at 460 nm and 470 nm, respectively, with large stopbands of >92 nm, and high reflectance of >95%. Though there is a small difference in the central wavelengths, the stopbands of the two DBRs have a sufficient overlap, allowing formation of optical modes in the green wavelength range. Further optimisation of the structures could enlarge the stopband overlap of the two DBRs. The overall reflectance of the microcavity is observed to have four dips, which agrees with several modes observed in both experimental and FDTD spectra, which will be discussed later in the paper.

Angled reflectivity measurements have been carried out at room temperature to investigate polariton characteristics in the microcavities. The microcavities are illuminated with a broadband unpolarised high-density plasma light source and a calibrated reflectance as a reference. The reflected light is collected into an Andor 500i monochromator and analysed with a Newton couple charged device (CCD). Figure 3(a) shows reflectance as a function of the varying angle for a microcavity between a NP-GaN/GaN DBR and a top dielctric DBR. The 0° angle means the direction perpendicular to the plane of the microcavity. An overall blue shift in emissions can be observed for all modes. However, the 2.95 eV (420 nm) mode becomes weaker before disappearing at around 60°. Figure 3(b) plots the photon energies of the modes as a function of the varying angle for the microcavity. It reveals a slight anti-crossing behaviour at 2.77 eV, where the upper and lower branches of the polariton begin to 'repel' each other after closing in. The photon energy, at which the mode disappears, can be used as the energy of the exciton. In this case, it is observed to be 2.77 eV. The energy of the photon can be determined by fitting the data with the coupled harmonic coupling model, as expressed by equation (1)

$$E_{\mathrm{LP}}E_{\mathrm{UP}} = \frac{1}{2}[E_{\mathrm{exe}} + E_{\mathrm{ph}} \pm \sqrt{\Omega^2 + (E_{\mathrm{exe}} + E_{\mathrm{ph}})^2} \qquad (1)$$

where Ω is Rabi splitting, $E_{\mathrm{LP}}E_{\mathrm{UP}}$ is energy of lower and upper branches, E_{exe} is energy of exciton during coupling, and E_{ph} is energy of photon where the anti-crossing begins [22]. The calculated curves for the upper and lower polariton (UP and LP) dispersion seem to fit the experimental data. In this work, the rabi splitting for the microcavities is 5 meV. A lot of similar studies have been performed while a major part focus on bulk GaN [22] or planar MQWs [23, 24]. Nevertheless, a work on GaN based microcavities has been reported to achieve a high Rabi splitting value of 30 meV [25]. To further increase the rabi splitting would require the optimisation between the cavity resonance and InGaN exciton.

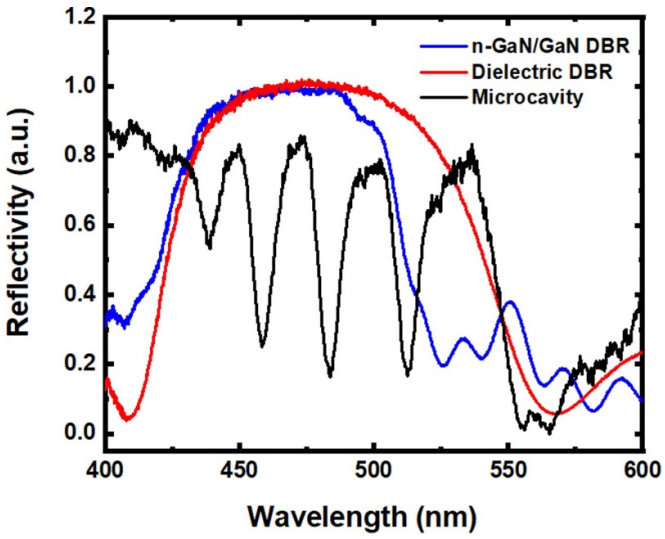

Figure 2. Reflectivity spectra of the microcavity, a lattice matched NP-GaN/GaN, and a dielectric DBR. Showing both have high reflectivity DBRs > 95% both covering a range between 480–500 nm. The combined cavity creates a reflectance spectrum with dips representing apparent modes.

Figure 3(c) presents the angular reflectivity of the microcavity without the top dielectric DBR. It has a larger separation compared to the microcavity with two DBRs, suggesting the increased cavity length when adding a top DBR. This is probably due to that the reflectivity of DBR becomes >95% midway through the DBR structure. Plotting of the mode energies against the angle is shown in figure 3(d). It exhibits a linear change in wavelength for both the two modes with a constant separation, proving that polariton only forms in the enhanced cavity. Demonstration of the polariton behaviour combined with the rabi splitting value indicates that the microcavity created along with a lattice-matched NP-GaN/GaN DBR and a top dielectric DBR is capable of high-quality confinement required for lasing behaviour [23].

Furthermore, power-dependent photoluminescence (PL) measurements are performed at room temperature to investigate optical characteristics of the microcavities with emphasis on its lasing properties. The measurements are carried out with a commercial confocal microscopy system equipped with a high-resolution x–y–z piezo-stage allowing the excitation and emission collection from a single micro disk device. The devices are non-resonantly excited using a 375 nm continuous wave laser, and the emission is then collected into a monochromator and detected with a CCD. The laser spot size allows for spatial resolution for up to 200 nm, approximately 100 nm in diameter. The emission exhibits a series of spectral peaks which are associated with optical modes. Figure 4(a) displays power-dependent PL spectra with excitation powers from 30 to 800 μW of the microcavity. The emission intensity increases

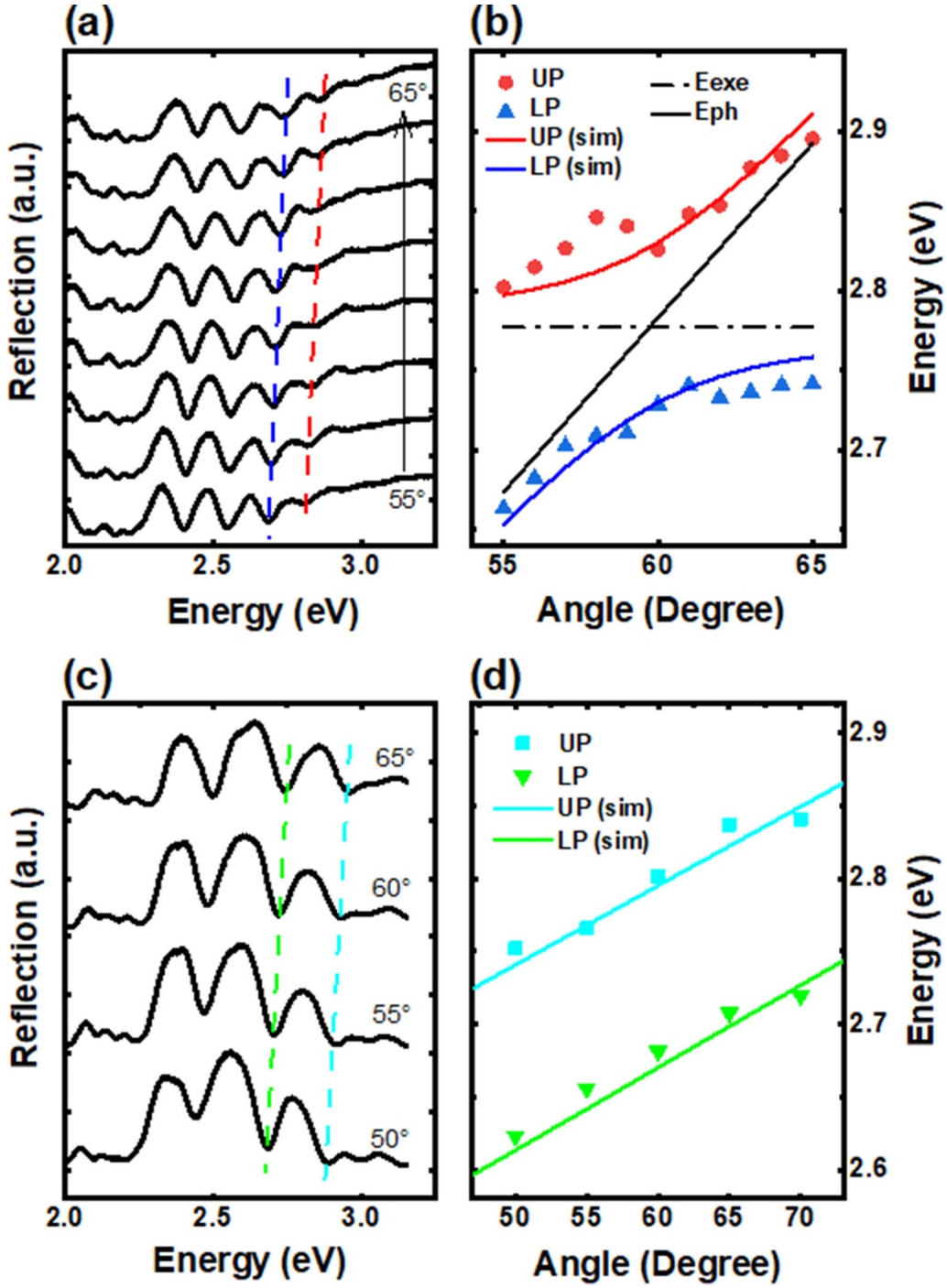

Figure 3. (a) Angular reflectivity spectra of the microcavity between a NP-GaN/GaN DBR and a dielectric DBR. (b) Photon energy vs angle of the microcavity bewteen a NP-GaN/GaN DBR and a dielectric DBR. (c) Angular reflectivity spectra of a micro cavity without a top DBR. (d) Photon energy vs angle of the microcavity without a top DBR.

constantly with the increase of the power. When the power is above a few hundred μW, the intensities of two emission peaks at 488 nm and 511 nm begin to go through a nonlinear change in the spectra, and both the two peaks are narrowing quickly.

It shows that the two main peaks are located at 488 nm and 511 nm with an approximately 20 nm separation. It does not agree with the theoretical spacing of vertical Fabre–Perot (FP), or circular WGMs for the microcavity between two DBRs, as estimated by equation (2).

$$\Delta\lambda = \frac{\lambda^2}{nL} \tag{2}$$

where λ is peak wavelength, n is refractive index, L is cavity length [19].

However, upon closer examination there are a few other modes, like modes at 479 nm, 502 nm and 523 nm with a smaller average separation of 11 nm, as shown in the inset detail. Combined with the main peaks, these could be ascribed to

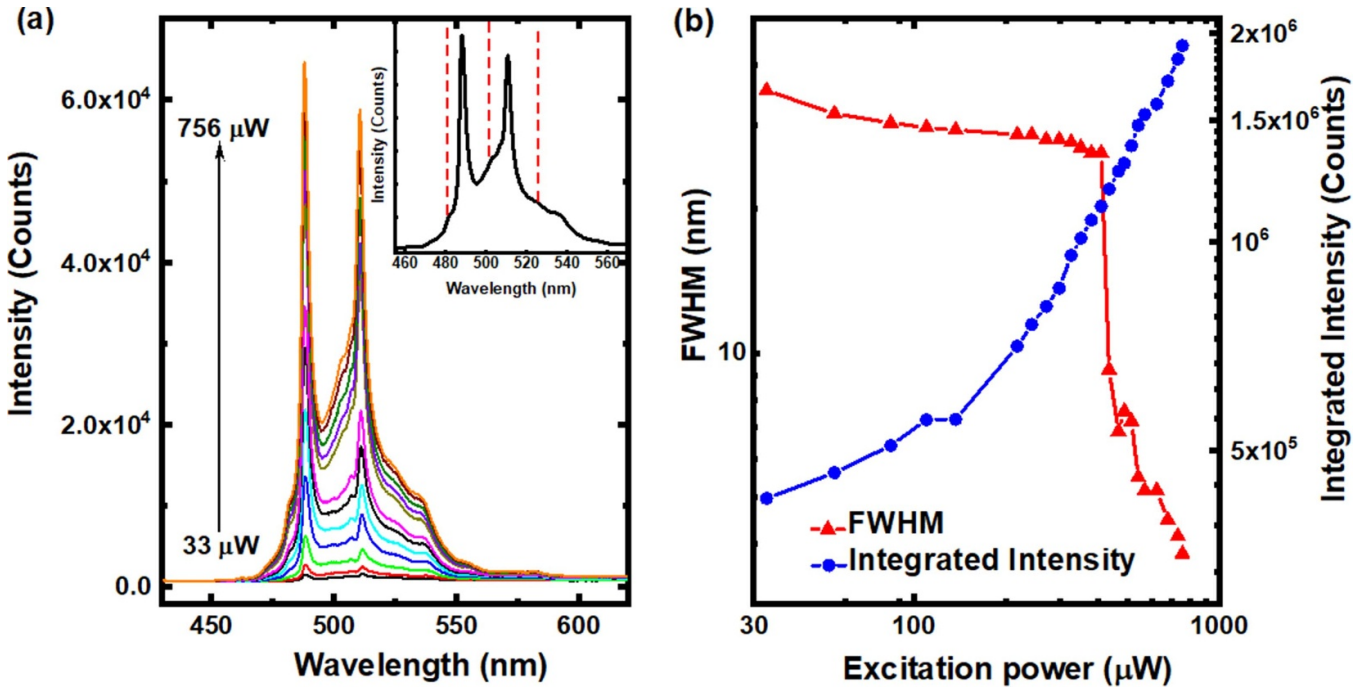

Figure 4. (a) Power-dependent photoluminescence spectra excited with powers from 30 μW to 800 μW of an InGaN/GaN microcavity. The main peak at 480 nm shows a dramatic increase in intensity from 410 μW. The inset shows smaller mode peaks of 479 nm, 502 nm and 523 nm in detail. (b) Integrated intensity and FWHM of the peak at 488 nm mode as a function of excitation power with a log-log scale.

WGMs from the circular confinement in the microcavity. The overlap between the two types of modes causes interference, making them hard to separate. Optimisation in the structure by supressing one set of modes could further enhance the emission. Based on the reflectivity measurements, the shorter peak could also be a polariton mode. At certain wavelengths, both types of mode could be formed, which can be separately activated by passing through different lasing thresholds [18]. This could explain why the sudden narrowing of the peak appears to happen twice while increasing with power in figure 4(a).

Figure 4(b) shows the integrated intensity and the full width half maximum (FWHM) of the peak at 488 nm as a function of excitation power with a log–log scale. It demonstrates a dramatic increase in the integrated intensity above a certain power threshold, which is a typical indicator of lasing behaviour [26]. The lasing threshold can be calculated to be 410 μW, corresponding to a power density of 40 kW cm^{-2}. Similar sized free standing micro disks as reported by Tabataba-Vakili *et al* have a threshold of 18 kW cm^{-2} though at a shorter wavelength [27]. This lasing threshold is higher compared to micro lasers in other reports, which can be attributed to the non-optimisation of the microstructure. It is noted that the FWHM shows a clear decreasing trend with increasing the power. Especially, the peak narrows dramatically from above 400 μW with the FWHM decreasing to 4 nm finally, which further confirms a stimulated emission [28].

The positions of modes within the microcavity have been calculated by standard FDTD simulations. For simulation, the electric field is injected by a plane wave source, which is placed above the top DBR, with an emission wavelength of 400–700 nm. The geometrical data of our devices are from the *in-situ* growth characterisation. Monitors, placed inside the cavity, are used to determine the decay in the electric field and the wavelengths of resonant modes. The boundary conditions are set as periodic on *X, Y* and perfectly matched layers in the *Z* dimension to reduce the simulation requirements. The effective indices of the nanoporous layers are approximated from the volume average theory using equation (3), as the scattering factor $\chi = \frac{\pi d}{\lambda} < 0.2$, where d is the diameter of the nanopore [8, 15, 29].

$$n_{\mathrm{por}} = \left[(1-\varphi)\, n_{\mathrm{GaN}}^2 + \varphi n_{\mathrm{air}}^2 \right]^{1/2} \tag{3}$$

where n_{por}, n_{GaN}, n_{air} and Φ are the effective refractive index of the nanoporous layer, refractive index of GaN, refractive index of air and porosity, respectively [30]. The porosity is assumed to be 0.5 from SEM images, leading to $n_{\mathrm{por}} = 1.9$.

Figure 5 displays both the WGM and the FP modes of the microcavity obtained by the FDTD simulation. The black arrows show the lasing modes of 488 nm and 511 nm, and some higher order modes. It shows that the positions of the simulated modes are in line with the stimulated emissions in the experimental spectra. In the simulation, the WGM and FP modes have an average separation of 8.7 nm and 34.8 nm, respectively. Compared to the simulated FP modes, the mode separation for the simulated WGM is closer to the experimental mode separation average of 11 nm. It is worth noting that between both the two mode systems have one mode at around 485 nm, which could lead to a competition, finally limiting the efficiency of the microcavity. Supressing one mode system by reducing the size (either radially

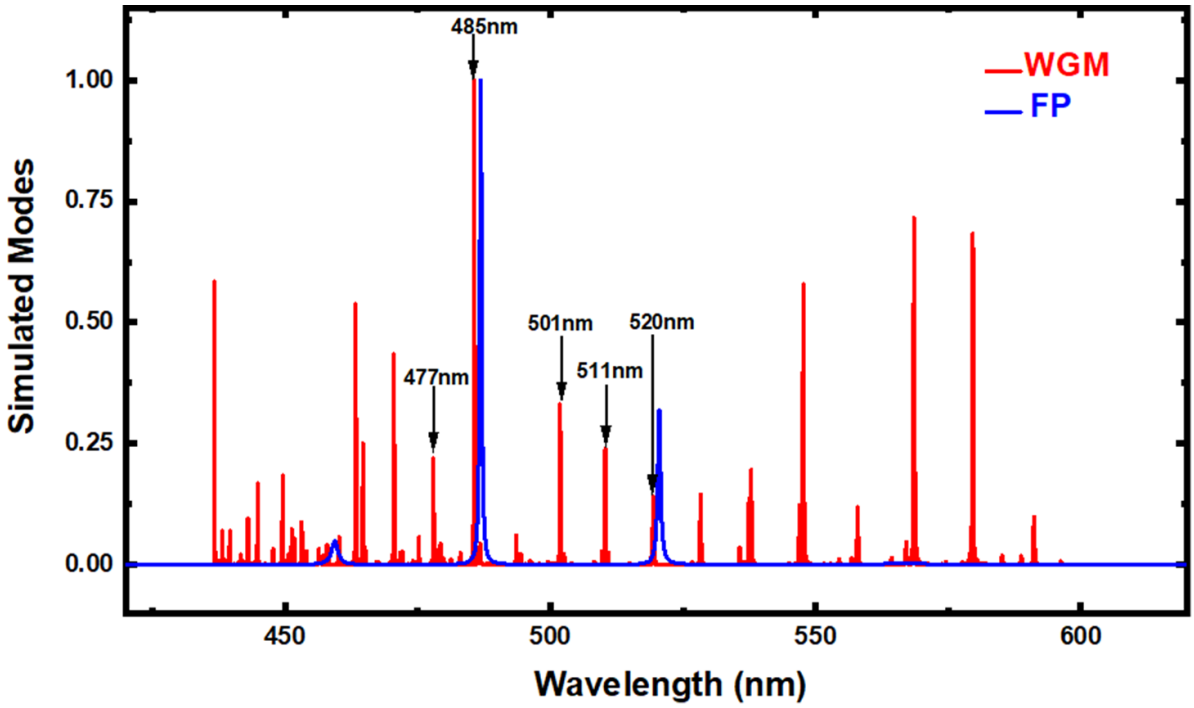

Figure 5. FDTD simulation of the microcavity showing FP and WGM modes. Black arrows show the lasing modes of 488 nm and 511 nm, and some higher order modes.

or vertically) should further improve the performance of the microcavity [31].

4. Conclusion

In this study, we have reported a new method of creating InGaN/GaN MQW microdisk arrays through overgrowth of MQWs on a patterned GaN template. Based on the microdisk array, a high quality microcavity has been achieved by forming a highly reflective lattice-matched NP-GaN/GaN DBR on bottom and a dielectric DBR on top. Optical pumping measurements have demonstrated a stimulated emission at 488 nm with a threshold of 410 μW. The 3D FTDT simulations are in good agreement with the experiment in terms of the mode positions. While the performance can be further enhanced with the structure optimisation, the InGaN-based microdisk arrays are great candidates for creating high quality microcavities with lasing properties.

Data availability statement

The data that support the findings of this study are available upon reasonable request from the authors.

Acknowledgments

Financial support is acknowledged from the Engineering and Physical Sciences Research Council (EPSRC), UK via EP/P006973/1, EP/M015181/1 and EP/P006361/1.

ORCID iDs

Jie Bai https://orcid.org/0000-0002-6953-4698
Tao Wang https://orcid.org/0000-0001-5976-4994

References

[1] Mei Y, Xie M C, Xu H, Long H, Ying L Y and Zhang B P 2021 Electrically injected GaN-based microdisk towards an efficient whispering gallery mode laser *Opt. Express* **29** 5598–606
[2] Wasisto H S, Prades J D, Gülink J and Waag A 2019 Beyond solid-state lighting: miniaturization, hybrid integration, and applications of GaN nano- and micro-LEDs *Appl. Phys. Rev.* **6** 41315
[3] Zhao C, Tang C W, Wang J and Lau K M 2020 Ultra-low threshold green InGaN quantum dot microdisk lasers grown on silicon *Appl. Phys. Lett.* **117** 031104
[4] Bai J, Cai Y, Feng P, Fletcher P, Zhu C, Tian Y and Wang T 2020 Ultrasmall, ultracompact and ultrahigh efficient InGaN micro light emitting diodes (μLEDs) with narrow spectral line width *ACS Nano* **14** 6906–11
[5] Haberer E, Sharma R, Meier C, Stonas A R, Nakamura S, DenBaars S P and Hu E L 2004 Free-standing, optically pumped, GaN/InGaN microdisk lasers fabricated by photoelectrochemical etching *Appl. Phys. Lett.* **85** 5179–81
[6] Choi H W, Hui K N, Lai P T, Chen P, Zhang X H, Tripathy S, Teng J H and Chua S J 2006 Lasing in GaN microdisks pivoted on Si *Appl. Phys. Lett.* **89** 211101
[7] Wang D, Zhu T, Oliver R A and Hu E L 2018 Ultra-low-threshold InGaN/GaN quantum dot micro-ring lasers *Opt. Lett.* **43** 799–802
[8] Mishkat-Ul-Masabih S, Luk T S, Rishinaramangalam A, Monavarian M, Nami M and Feezell D 2018 Nanoporous distributed Bragg reflectors on free-standing nonpolar m-plane GaN *Appl. Phys. Lett.* **112** 041109

[9] Seong T-Y and Amano H 2020 Surface passivation of light emitting diodes: from nano-size to conventional mesa-etched devices *Surf. Interfaces* **21** 100765
[10] Lu S, Li J, Huang K, Liu G, Zhou Y, Cai D, Zhang R and Kang J 2021 Designs of InGaN micro-LED structure for improving quantum efficiency at low current density *Nanoscale Res. Lett.* **16** 99
[11] Rousseau I, Callsen G, Jacopin G, Carlin J-F, Butté R and Grandjean N 2018 Optical absorption and oxygen passivation of surface states in III-nitride photonic devices *J. Appl. Phys.* **123** 113103
[12] Zhao C *et al* 2015 An enhanced surface passivation effect in InGaN/GaN disk-in-nanowire light emitting diodes for mitigating Shockley–Read–Hall recombination *Nanoscale* **7** 16658–65
[13] Wang J, Feng M, Zhou R, Sun Q, Liu J, Sun X, Zheng X, Ikeda M, Sheng X and Yang H 2020 Continuous-wave electrically injected GaN-on-Si micro disk laser diodes *Opt. Express* **28** 12201–8
[14] Esendag V *et al* 2021 Investigation of electrical properties of InGaN-based micro-light-emitting diode arrays achieved by direct epitaxy *Phys. Status Solidi* a **218** 2100474
[15] Zhang C, Park S H, Chen D, Lin D-W, Xiong W, Kuo H-C, Lin C-F, Cao H and Han J 2015 Mesoporous GaN for photonic engineering—highly reflective GaN mirrors as an example *ACS Photonics* **2** 980–6
[16] ElAfandy R T, Kang J-H, Li B, Kim T K, Kwak J S and Han J 2020 Room-temperature operation of c-plane GaN vertical cavity surface emitting laser on conductive nanoporous distributed Bragg reflector *Appl. Phys. Lett.* **117** 011101
[17] Yuan G, Zhang C, Xiong K and Han J 2018 InGaN/GaN microdisks enabled by nanoporous GaN cladding *Opt. Lett.* **43** 5567–70
[18] Xie Z L *et al* 2007 High reflectivity AlGaN/AlN DBR mirrors grown by MOCVD *J. Cryst. Growth* **298** 691
[19] Zhu G, Li J, Zhang N, Li X, Dai J, Cui Q, Song Q, Xu C and Wang Y 2020 Whispering-gallery mode lasing in a floating GaN microdisk with a vertical slit *Sci. Rep.* **10** 253
[20] Tawara T, Gotoh H, Akasaka T, Kobayashi N and Saitoh T 2004 Observation of InGaN cavity polaritons at room temperature *Conf. on Lasers and Electro-Optics/Int. Quantum Electronics Conf. and Photonic Applications Systems Technologies Technical Digest (CD) Optical Society of America* p IThB1
[21] Shi X, Long H, Wu J, Chen L, Ying L, Zheng Z and Zhang B 2019 Theoretical optimization of inhomogeneous broadening in InGaN/GaN MQWs to polariton splitting at low temperature *Superlattices Microstruct.* **128** 151–6
[22] Wu J, Shi X, Long H, Chen L, Ying L, Zheng Z and Zhang B 2019 Large Rabi splitting in InGaN quantum wells microcavity at room temperature *Mater. Res. Express* **6** 076204
[23] Wu J Z, Long H, Shi X, Luo S, Chen Z, Feng Z, Ying L, Zheng Z and Zhang B 2019 Polariton lasing in InGaN quantum wells at room temperature *Opto-Electron. Adv.* **2** 190014
[24] Faure S, Guillet T, Lefebvre P, Bretagnon T and Gil B 2008 Comparison of strong coupling regimes in bulk GaAs, GaN, and ZnO semiconductor microcavities *Phys. Rev.* B **78** 235323
[25] Malpuech G, Di Carlo A, Kavokin A, Baumberg J J, Zamfirescu M and Lugli P 2002 Room-temperature polariton lasers based on GaN microcavities *Appl. Phys. Lett.* **81** 412–4
[26] Athanasiou M, Smith R M, Pugh J, Gong Y, Cryan M J and Wang T 2017 Monolithically multi-color lasing from an InGaN microdisk on a Si substrate *Sci. Rep.* **7** 10086
[27] Tabataba-Vakili F *et al* 2020 Analysis of low-threshold optically pumped III-nitride microdisk lasers *Appl. Phys. Lett.* **117** 121103
[28] Ghosh P, Yu D, Li G, Huang M and Liu Y 2021 Size dependent polaritonic effects in GaN microrod studied through optical property investigation *Optik* **240** 166829
[29] Braun M M and Pilon L 2006 Effective optical properties of non-absorbing nanoporous thin films *Thin Solid Films* **496** 505–14
[30] Zhang X, Cheung Y F, Zhang Y and Choi H W 2014 Whispering-gallery mode lasing from optically free-standing InGaN microdisks *Opt. Lett.* **39** 5614–7
[31] Sellés J *et al* 2016 Deep-UV nitride-on-silicon microdisk lasers *Sci. Rep.* **6** 21650